Science of the Total Environment 858 (2023) 159972

Contents lists available at ScienceDirect

Science of the Total Environment

journal homepage: www.elsevier.com/locate/scitotenv

Increases in ozone-related mortality in China over 2013–2030 attributed to historical ozone deterioration and future population aging

Lei Chen [a,b,c], Hong Liao [a,*], Jia Zhu [a], Ke Li [a], Yang Bai [a], Xu Yue [a], Yang Yang [a], Jianlin Hu [a], Meigen Zhang [b,d]

[a] Jiangsu Key Laboratory of Atmospheric Environment Monitoring and Pollution Control, Jiangsu Collaborative Innovation Center of Atmospheric Environment and Equipment Technology, School of Environmental Science and Engineering, Nanjing University of Information Science and Technology, Nanjing 210044, China
[b] State Key Laboratory of Atmospheric Boundary Layer Physics and Atmospheric Chemistry, Institute of Atmospheric Physics, Chinese Academy of Sciences, Beijing 100029, China
[c] State Environmental Protection Key Laboratory of Sources and Control of Air Pollution Complex, Beijing 100084, China
[d] University of Chinese Academy of Sciences, Beijing 100049, China

HIGHLIGHTS

- Past and future changes in O_3-mortality and respective leading cause are examined.
- During 2013–2019, national O_3-mortality exhibits a trend of +14.1 thousand yr^{-1}.
- The O_3 air quality deterioration contributes 90.1 % of 2013–2019 O_3-mortality rise.
- From 2019 to 2030, national O_3-mortality will increase by 50.4–103.7 thousand.
- Population aging will become the primary cause of future O_3-mortality rises.

GRAPHICAL ABSTRACT

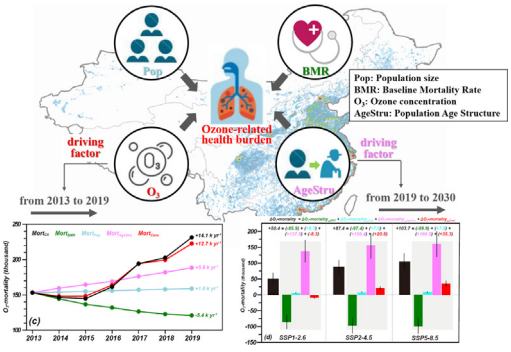

ARTICLE INFO

Editor: Jianmin Chen

Keywords:
Ozone air quality
Long-term exposure
Health burden
Population aging
Historical and future change

ABSTRACT

We systematically examine historical and future changes in premature respiratory mortalities attributable to ozone (O_3) exposure (O_3-mortality) in China and identify the leading cause of respective change for the first time. The historical assessment for 2013–2019 is based on gridded O_3 concentrations generated by a multi-source-data-fusion algorithm; the future prediction for 2019–2030 uses gridded O_3 concentrations projected by four Coupled Model Intercomparison Project Phase 6 (CMIP6) models under three Shared Socioeconomic Pathways (SSP) scenarios. During 2013–2019, national annual O_3-mortality is 176.3 thousand (95%CI: 123.5–224.0 thousand) averaged over 2013–2019 with an increasing trend of 14.1 thousand yr^{-1} (95%CI: 10.2–17.4 thousand yr^{-1}); sensitivity experiments show that the O_3-mortality varies at a rate of +12.7 (95%CI: 9.2–15.6), +5.8 (95%CI: 4.0–7.4), +1.0 (95% CI: 0.7–1.2), −5.4 (95%CI: −6.9 to −3.7) thousand yr^{-1}, owing to changes in O_3 concentration, population age structure, population size, mortality rate for respiratory disease, respectively. The deterioration of O_3 air quality, shown as significant increase in O_3 concentration, is identified as the primary factor which contributes 90.1 % of 2013–2019 O_3-mortality rise. Compared with O_3-mortality estimated in this study, the widely-used O_3-mortality assessment method based on urban-site-dominant O_3 measurements generates close national O_3-mortality but overestimates (underestimates) provincial O_3-mortality in coastal (central) provinces. From 2019 to 2030, national O_3-mortality is projected to increase by 50.4–103.7 thousand under different SSP scenarios. The change in age structure (i.e. population aging) alone will result in significant O_3-mortality rises of 137.9–160.5 thousand. Compared with 2013–2019 rapid O_3 increase (+2.5 μg m^{-3} yr^{-1} at national level), O_3 concentrations are projected to increase at a lower rate

* Corresponding author.
E-mail address: hongliao@nuist.edu.cn (H. Liao).

http://dx.doi.org/10.1016/j.scitotenv.2022.159972
Received 31 July 2022; Received in revised form 18 October 2022; Accepted 1 November 2022
Available online 8 November 2022

(+0.4 μg m^{-3} yr^{-1} in SSP5–8.5) or even decrease (−0.7 μg m^{-3} yr^{-1} in SSP1-2.6) from 2019 to 2030. Therefore, population aging, in place of O_3 air quality deterioration, will become the leading cause of future O_3-mortality rises during the coming decade.

1. Introduction

China has witnessed significant $PM_{2.5}$ declines and rapid O_3 rises since the implementation of a series of drastic air pollution control measures in 2013. The national population–weighted $PM_{2.5}$ concentration decreased by 32 % during 2013–2017 (Zhang et al., 2019), while the population–weighted O_3 concentration increased with a rate of +2.1 μg m^{-3} yr^{-1} at the national level during the five years (Xue et al., 2020). Now O_3 is replacing $PM_{2.5}$ as the primary pollutant during summer in most regions of China. Previous studies have confirmed that exposure to O_3 can cause respiratory diseases (Jerrett et al., 2009; Anenberg et al., 2010; Liu et al., 2018; Xie et al., 2019; Zhong et al., 2019; Yin et al., 2020; Chen et al., 2021; Guo et al., 2021). However, compared with the massive focuses on the health benefits from improved $PM_{2.5}$ air quality (Xue et al., 2019; Zhang et al., 2019; Zheng et al., 2019; Chen et al., 2020; Jiang et al., 2020; Yue et al., 2020), less attention is paid to the increased health burden caused by worsened O_3 pollution (Madaniyazi et al., 2016; Lu et al., 2020; Wang et al., 2020; Zhang et al., 2021).

Health burden assessment of O_3 exposure firstly depends on the acquisition of O_3 concentration. Up to now, O_3 concentration over China can be obtained from the Chinese nationwide air quality monitoring network, satellite retrievals, numerical simulations, and multi-source data fusion models. In situ O_3 observations from the China National Environmental Monitoring Centre (CNEMC) became available in 2013 and have been used to evaluate O_3 pollution and associated health impacts in China since then (Lu et al., 2018, 2020; Feng et al., 2019; Chen et al., 2020; Maji and Namdeo, 2021; Wang et al., 2021). However, over 90 % of CNEMC monitoring sites are located in urban areas which only account for 2 % of the whole country's area and 50 % of the national total population (Gao et al., 2020; Kong et al., 2021), leading to possible deviations when the urban-site-dominant observations are used to assess the health risks from O_3 exposure at a national or provincial level (Chen et al., 2019; Gao et al., 2020; Malashock et al., 2022). Gridded data from satellite retrievals and numerical simulations provide a relatively complete spatial coverage of O_3 concentration. However, most remote sensing products of O_3 are column concentrations which are less indicative of surface-layer pollution. Although satellite observations have been shown to have some sensitivity to boundary layer O_3 pollution, they have deviations because of weak retrieval sensitivity and larger upper tropospheric variability in certain places as well as susceptibility to meteorological factors (Liang et al., 2019; Shen et al., 2019). Numerical simulations, including simple statistical models and/or complex chemical transport models, generally predict underestimated/overestimated surface-layer O_3 due to the uncertainties brought by emission inventories and O_3 photochemistry (Travis et al., 2016; Li et al., 2019; Marco et al., 2022). More recently, a data-fusion algorithm for O_3 estimation that combines in situ observations, satellite remote sensing measurements, and model simulations was developed (Xue et al., 2020; Xiao et al., 2022); the corresponding database named "Tracking Air Pollution in China" (TAP) was released and provided gridded ground-layer O_3 concentrations over China since 2013. The TAP database exhibits excellent performance on observed O_3 concentrations. With a more complete spatiotemporal coverage, the TAP O_3 database, therefore, is suitable for applying to O_3 health assessment.

Projecting future O_3 concentration is essential for future O_3 health burden assessment. Numerical model is the most common way to predict future O_3 concentrations. Earlier modeling studies to project future O_3 concentrations generally used the Intergovernmental Panel on Climate Change (IPCC) Special Report on Emissions Scenarios (SRES) that were designed for the IPCC Fourth Assessment Report (Wang et al., 2013; Zhu et al., 2017), and Representative Concentration Pathways (RCPs) emissions scenarios that were developed for the Fifth Coupled Model Intercomparison Project (CMIP5) simulations in support of the IPCC Fifth Assessment Report (Zhu and Liao, 2016; Meehl et al., 2018). More recently, the Coupled Model Intercomparison Project Phase 6 (CMIP6) provides an opportunity to update the assessment of future air quality by using the latest generation of climate and Earth System Models. A new set of future scenarios named Shared Socioeconomic Pathways (SSPs) that are generated for CMIP6 indicate a wide range of trajectories in climate change and emissions, and allow for an improved analysis of future air quality (Gidden et al., 2019). Turnock et al. (2020) made a first assessment of historical and future surface O_3 changes over different world regions under different SSPs. Since China has witnessed rapid O_3 rises since 2013, it is of interest to project future O_3 levels and associated health burden in the coming decade under the new SSPs with a special focus on China.

Besides air pollutant concentration, changes in population size, population age structure, and death rate of diseases also contribute to the changes in mortality attributable to ambient air quality (Cohen et al., 2017; Sicard et al., 2021). During the past decade, China's total population has grown by 4.9 % and the proportion of the elderly over 65 years old has increased from 8.5 % to 12.6 % over 2009–2019 (China's National Bureau of Statistics 2020, 2020). The baseline mortality rate for respiratory disease in China has been declining owing to improving medical conditions (http://ghdx.healthdata.org/gbd-results-tool). According to World Population Prospects 2019, China's population will peak in 2030 with rapid population aging (https://population.un.org/wpp/). The future mortality rate for respiratory disease over China will also show large decreases in 2030 (Li et al., 2017). Although several studies have quantified the contributions of changes in these factors to the change in $PM_{2.5}$-related mortality over China (Ding et al., 2019; Yue et al., 2020; Geng et al., 2021), the cause assessment for O_3-related mortality change, both for the past and the future, is very limited. Quantitatively distinguishing the factors driving changes in O_3-related mortality is helpful to identify the challenges that must be overcome to reduce the public health impact of exposure to O_3 pollution.

This study aims to (1) obtain the spatiotemporal characteristics of O_3-related health impacts in China during 2013–2019, based on gridded O_3 concentration provided by a newly developed database named TAP; (2) quantify the relative contributions of four underlying driving factors (population size, population age structure, mortality rate for respiratory disease, and O_3 concentration) to the changes in premature respiratory mortalities attributable to long-term O_3 exposure (thereafter denoted as O_3-mortality) in China during 2013–2019; (3) predict future changes in O_3-mortality under SSP scenarios based on gridded O_3 concentration projected by CMIP6 and distinguish the respective contribution of each factor over China from 2019 to 2030.

2. Materials and methods

2.1. Ozone concentration

The O_3 concentration over China during 2013–2019 is estimated by a data-fusion algorithm that combines in situ observations, satellite remote sensing measurements, and WRF-CMAQ model results (Xue et al., 2020; Xiao et al., 2022). The O_3 database named "Tracking Air Pollution in China" (TAP) has a horizontal resolution of 0.1° × 0.1° and can be publicly accessed from http://tapdata.org.cn/. Detailed data fusion steps can be found in Xue et al. (2020) and Xiao et al. (2022). Compared with in situ observations and satellite measurements, the gridded O_3 data has a more complete spatiotemporal coverage; compared with model simulations, the O_3

data based on multi-source data fusion exhibits more excellent performance on O_3 concentration. Given above advantages and latest study period, the state-of-the-art O_3 estimates are chosen to support health assessment since China's clean air actions in this study. We conduct comparisons of TAP versus CNEMC O_3 concentrations in Fig. 1. The observed O_3 concentrations from CNEMC can be obtained at http://106.37.208.233:20035/. The calculated normalized mean bias (NMB) is smaller than 1 % and index of agreement (IOA) is larger than 0.9 for each year, verifying the high performance of TAP O_3 database.

Future O_3 concentrations in 2030 are taken from CMIP6 simulations under different SSP scenarios. It is noted that the O_3 concentration in year 2030 is very close to the mean value during 2026–2034; their differences are less than ±0.6 %. Therefore, the concentration in year 2030 can represent the multi-year mean O_3 level to some extent. The SSPs used in CMIP6 projections represent an update from the RCPs used in CMIP5 experiments as they include socioeconomic development pathways with aims to achieve a certain level of climate mitigation (van Vuuren et al., 2014; Riahi et al., 2017). The future projections in this study are based on three different SSP scenarios (SSP1-2.6 (strong-mitigation scenario), SSP2-4.5 (middle-of-the-road scenario), and SSP5-8.5 (weak-mitigation scenario)) and four CMIP6 models (BCC-CSM2-MR, GFDL-ESM4, MPI-ESM1-2-HR, NorESM2-MM) which have a horizontal resolution of 100 km. For consistency, the future O_3 data are regridded into 0.1° × 0.1° by using bilinear interpolation.

2.2. Population and age structure

We use a combination of gridded population data from LandScan (https://landscan.ornl.gov/) and provincial population data from China Statistical Yearbook (CSY, http://www.stats.gov.cn/tjsj/ndsj/) to obtain gridded and age-specific population data over China for years 2013–2019. The gridded population data over 2013–2019 with a horizontal resolution of 1 km are regridded to 0.1° × 0.1° to keep consistent with concentration data. All gridded population data in a province are multiplied by a factor which is the proportion of provincial population provided by CSY to the sum of gridded population in corresponding province. The national-level age-specific (eighteen age groups, 0–4, 5–9, …, 80–84, 85 +) population proportions provided by CSY are also applied to each grid to generate the final gridded and age-specific population data we want. Fig. 5(a) shows the yearly variations in Chinese population and its age structure. The future national-level population and age structure data in year 2030 are derived from Population Pyramid (https://www.populationpyramid.net/china/2030/). Assuming the proportions of population in a grid to total Chinese population are constant from 2019 to 2030, the gridded and age-specific population for year 2030 can be obtained through multiplying the national-level age-specific population in 2030 by the proportions in 2019.

2.3. Baseline mortality rate

The annual national-level age-specific and disease-specific baseline mortality rates (BMR) are obtained from Global Health Data Exchange (http://ghdx.healthdata.org/gbd-results-tool). We collect China's age-specific BMR data of chronic respiratory disease (CRD) from 2013 to 2019 in Fig. 5(b). Future BMR projections of CRD for the year 2030 are taken from WHO Global Health Estimates (https://colinmathers.com/2022/05/10/projections-of-global-deaths-from-2016-to-2060/). Some corrections in future BMR data are made according to scaling factors derived from the comparisons between historical BMRs in the year of 2016 from Global Health Data Exchange and WHO Global Health Estimates. Briefly, in the correction step, we first collect BMRs in year 2016 from Global Health Data Exchange and WHO Global Health Estimates. Then we compare the WHO BMR date with the corresponding value derived from GBD in each age group. Finally, the scaling factors are adopted to the future BMR in year 2030, assuming that historical biases persist in the future. It is noted that future age-specific BMR data for the adults above 30 are

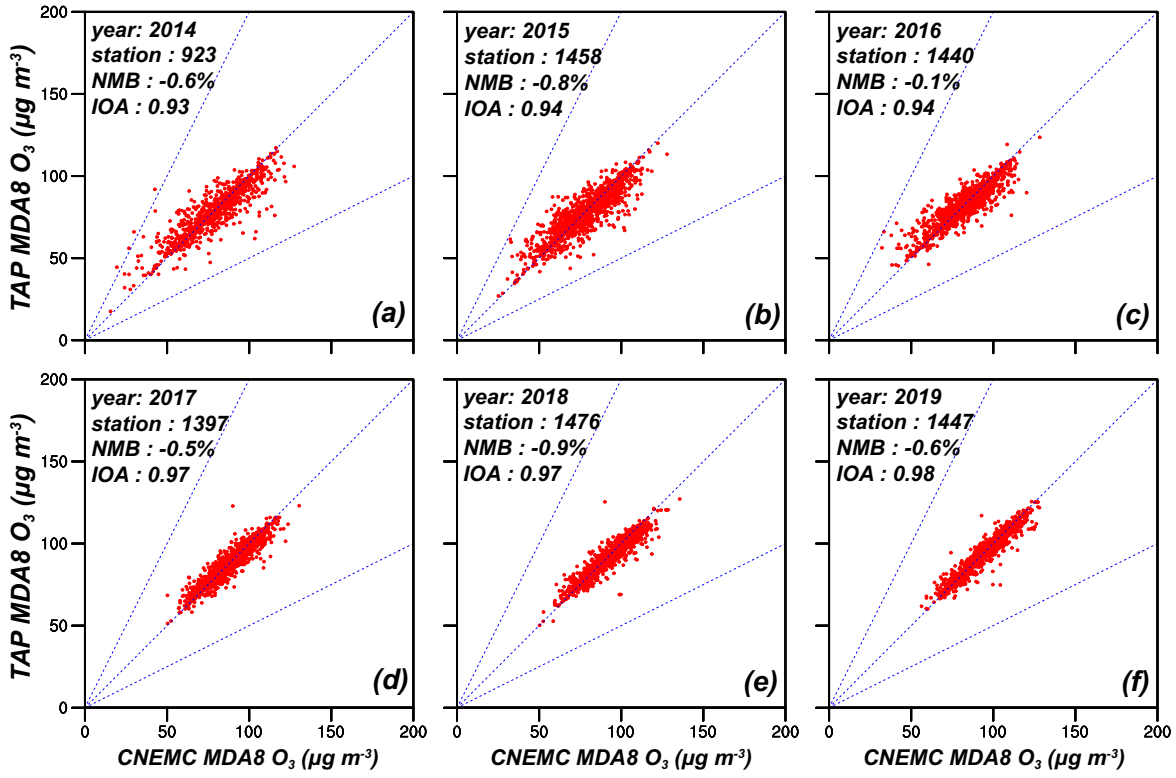

Fig. 1. Comparisons of annual mean TAP O_3 concentrations versus CNEMC O_3 concentrations at all CNEMC sites during 2014–2019. The TAP O_3 concentration is the derived one at the grid which corresponding CNEMC site locates. The comparison for year 2013 is not conducted because of the unavailability of partial CNEMC O_3 data in 2013. Also shown in each panel are the 1:1, 1:2, 2:1 lines, number of stations, normalized mean bias (NMB), and index of agreement (IOA).

divided into three age groups (30–49, 50–69, 70 +) rather than twelve age groups (30–34, 35–39, 40–44, …, 85 +) for history BMR data.

2.4. Ozone metrics relevant to human health

Ozone metrics relevant to human health impacts mainly focus on different parts of distributions of ozone concentrations (Lefohn et al., 2018). Some exposure metrics are used to assess health effects under relatively higher ozone values, while others focus on a combination of various parts of ozone distributions. Four metrics are analyzed in this study to characterize ozone pollution and their impacts on human health, including:

- AVGMDA8, an epidemiological metric that focuses on chronic exposure, which is defined as the annual mean of maximum daily 8-h average (MDA8) O_3 (WHO, 2006);
- 4MDA8, an exposure metric that focuses on higher O_3 concentrations, which is defined as the 4th highest MDA8 O_3 value over the entire year (US Federal Register, 2015);
- NDGT70, an exposure metric that focuses on high and mid-level O_3 concentrations, which is defined as the number of exceedances of MDA8 O_3 >70 ppb per year (US Federal Register, 2015);
- SOMO10, an exposure metric that focuses on high-, mid-, and low-level O_3 concentrations, which is defined as the annual sum of the positive differences between MDA8 O_3 and the cutoff value set at 10 ppb calculated for all days in a year (REVIHAAP, 2013).

The epidemiological metric (AVGMDA8) characterizes human health responses to long-term ozone exposure, and the premature respiratory mortality attributable to long-term ozone exposure are calculated by this metric. As Lefohn et al. (2018) emphasized that a common increase/decrease in ozone concentration could result in dissimilar changes in health metrics due to their different concerns on low, middle, or high ozone concentrations. So the three metrics of 4MDA8, NDGT70, and SOMO10 are selected to describe potential impacts of ozone on human health under different pollution levels.

2.5. Premature respiratory mortality attributable to long-term ozone exposure

We estimate premature respiratory mortality attributable to long-term ozone exposure (O_3-mortality) using the following equation (Eq. (1)), which has been widely used to estimate annual O_3-related mortality (Malley et al., 2017; Lin et al., 2018):

$$Mort_{d,t} = \sum_a \left[BMR_{a,d,t} \times \left(Pop_t \times AgeStru_{a,t} \right) \times AF_{d,t} \right] \quad (1)$$

where $Mort_{d,t}$ is the excess death due to O_3 exposure, $BMR_{a,d,t}$ is the baseline mortality rate of disease d for people within age group a in year t, Pop_t is the total population in year t, $AgeStru_{a,t}$ is the proportion of the population within age group a in year t, and $AF_{d,t}$ is the attributable fraction caused by disease d in year t defined as $AF_{d,t} = 1 - 1/RR_{d,t}$. $RR_{d,t}$ refers to the relative risk (RR) of cause-specific (disease d) death attributable to the change in O_3 concentration in year t, which can be calculated as the concentration-response function (CRF) as follows:

$$RR_{d,t} = exp^{\beta_d (Conc_t - Conc_0)} \quad (2)$$

for adults ≥ 30 years old. Here β_d is the concentration response factor which indicates that a 10-ppb increase in annual mean MDA8 O_3 concentration is associated with a 12 % (95 % Confidence Interval: 8–16 %) increase in RR of CRD (Turner et al., 2016); $Conc_t$ is annual mean MDA8 O_3 concentration in year t; $Conc_0$ is the threshold concentration which equals to 26.7 ppb as did in Malley et al. (2017) and Wang et al. (2020). In this study, we estimate O_3-mortality due to all chronic respiratory diseases, which means that disease d is CRD. Following Dang and Liao (2019) and Silva et al. (2016), we calculate uncertainties from 1000 Monte Carlo simulations that randomly sampled from normal distribution of the concentration response factor β_d.

2.6. Driving factor decomposition for historical and future O_3-mortality

The estimation for O_3-mortality (i.e., Eq. (1)) indicates that premature deaths are determined by baseline mortality rate (BMR), population (Pop), age structure (AgeStru), and O_3 concentration (Conc). We perform five sets of experiments as shown in Table 1 to evaluate individual contribution of each factor to O_3-mortality variations during 2013–2019. Experiment "$Mort_{Ctl}$" represents the normal condition under which all factors are changed over 2013–2019. The mortality variations owing to BMR (Pop, AgeStru, Conc) variations alone are quantified by changing BMR (Pop, AgeStru, Conc) over 2013–2019 but keeping other factors fixed in corresponding experiment "$Mort_{BMR}$" ("$Mort_{Pop}$", "$Mort_{AgeStru}$", "$Mort_{Conc}$"). The similar experimental design is also applied to future O_3-mortality changes. For each SSP scenario, one normal experiment for present day (with all factors at 2019 levels) and five experiments for future (one normal experiment with all factors at 2030 levels and four sensitivity experiments in which one factor is at 2030 level but other three factors are kept at 2019 levels) are conducted.

3. Results and discussion

3.1. Spatiotemporal characteristics of ozone-related health burden during 2013–2019

3.1.1. Ozone metrics relevant to human health based on TAP database

The spatiotemporal characteristics of four ozone-health-related metrics, including AVGMDA8, 4MDA8, NDGT70, and SOMO10, are shown in Fig. 2. The four metrics, which have been introduced in Section 2.4, are generally used to assess health impacts of O_3 exposure and make health-related policies (Lefohn et al., 2018; Fleming et al., 2018; Xu et al., 2020). Fig. 2(a1–d1) show the spatial distributions of 2013–2019 means of the four metrics over China. All metrics exhibit the maximum values over North China Plain; high values of AVGMDA8 and SOMO10, two metrics focusing on the mean O_3 level and a combination of various parts of O_3 distribution (see Section 2.4), are also distributed over the northwestern China. The national average AVGMDA8, 4MDA8, NDGT70, and SOMO10 are calculated to be 81.9 μg m^{-3}, 127.9 μg m^{-3}, 2.0 days, and 6.9 mg m^{-3} day, respectively. The 2013–2019 trends of the four metrics over China are exhibited in Fig. 2(a2–d2). Increasing trends of all four metrics are observed across almost the whole China; the seven-year trends of the four metrics over China are + 2.5 μg m^{-3} yr^{-1}, + 3.8 μg m^{-3} yr^{-1}, + 0.5 days yr^{-1}, and + 0.3 mg m^{-3} days yr^{-1}, respectively. The maximum values of seven-year trends are located over North China Plain for all four metrics; the phenomenon is more pronounced for 4MDA8 and NDGT70 which focus on

Table 1
Experimental design for examining individual contribution of each factor to O_3-mortality variations during 2013–2019.

Experiment	Baseline mortality rate (BMR)	Population (Pop)	Age structure (AgeStru)	Concentration (Conc)	Purpose
$Mort_{Ctl}$	2013–2019	2013–2019	2013–2019	2013–2019	Mortality variations during 2013–2019
$Mort_{BMR}$	2013–2019	Fixed at 2013	Fixed at 2013	Fixed at 2013	Mortality variations owing to BMR variations alone
$Mort_{Pop}$	Fixed at 2013	2013–2019	Fixed at 2013	Fixed at 2013	Mortality variations owing to Pop variations alone
$Mort_{AgeStru}$	Fixed at 2013	Fixed at 2013	2013–2019	Fixed at 2013	Mortality variations owing to AgeStru variations alone
$Mort_{Conc}$	Fixed at 2013	Fixed at 2013	Fixed at 2013	2013–2019	Mortality variations owing to Conc variations alone

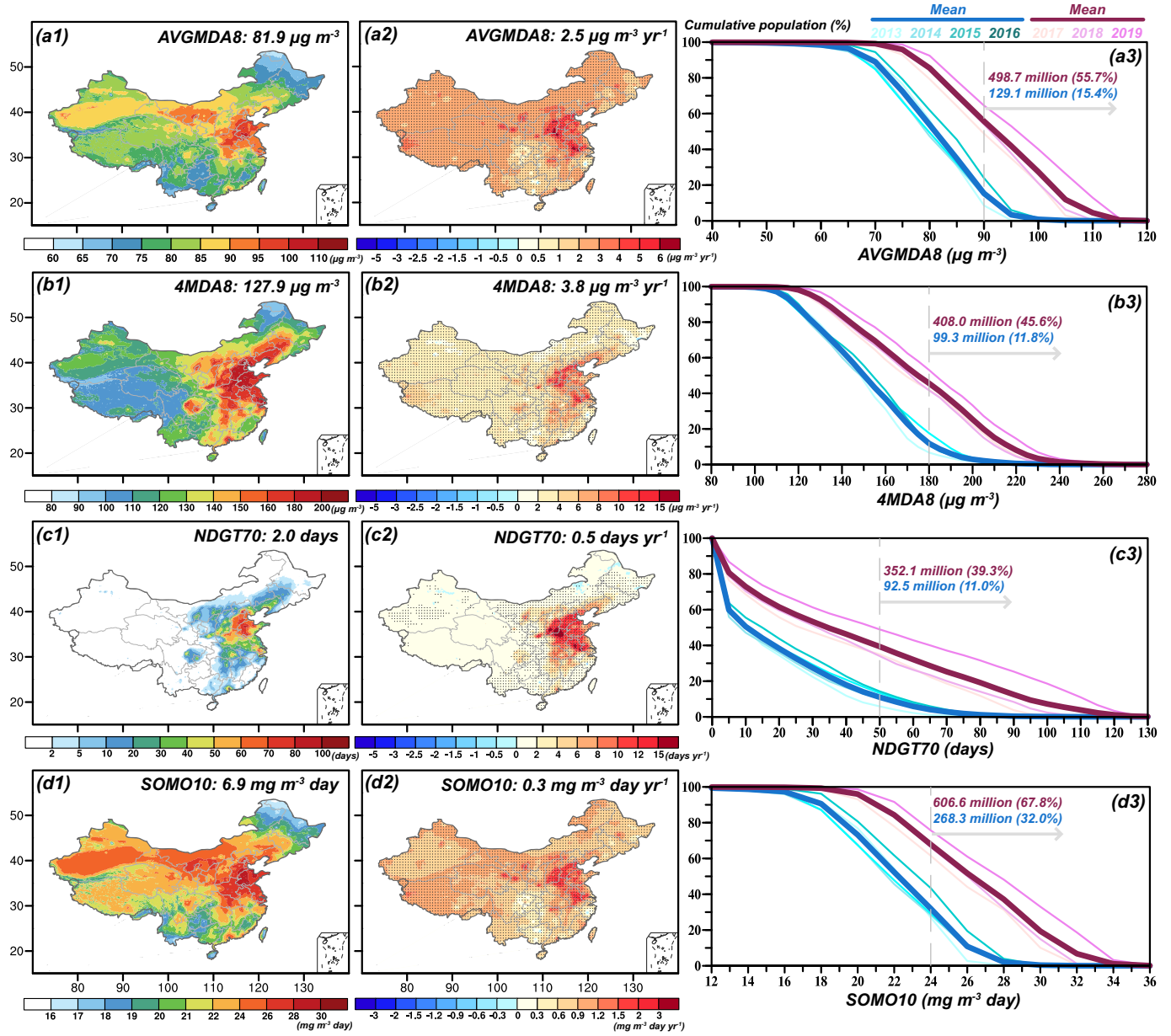

Fig. 2. Spatial distributions of 7-year (a1–d1) mean and (a2–d2) trend in four ozone metrics (AVGMDA8, 4MDA8, NDGT70, and SOMO10) during 2013–2019 over China. (a3–d3) Population exposure (adults above 30 years old) to O_3 pollution denoted by four metrics for each year during 2013–2019. Statistically significant trends with 95 % confidence level are marked with dots in (a2–d2). The metric values and trends averaged over China are shown at the top of each panel in (a1–d1) and (a2–d2). Population exposure curves for individual years during 2013–2019 are shown by light thin lines while the curves averaged for 2013–2016 (2017–2019) are represented by dark thick blue (red) lines in (a3–d3).

high and mid-level O_3 concentrations. The national AVGMDA8 trend estimated in this study (i.e. $+2.5$ μg m^{-3} yr^{-1}) is quite close to that in Xiao et al. (2022) who reported a trend of $+2.48$ μg m^{-3} yr^{-1}; the AVGMDA8 trend also exhibits the similar spatial distribution (Fig. 2(a2)) as that in Xue et al. (2020).

For further analysis on health impacts, Fig. 2(a3–d3) depict population exposure to O_3 pollution denoted by four metrics for each year during 2013–2019. For each metric, the curves gradually move to the right from 2013 to 2019, robustly confirming the deterioration of O_3 pollution and amplification of related health outcomes. The population percentage exposed to air with AVGMDA8 larger than 90 μg m^{-3} (4MDA8 > 180 μg m^{-3}, NDGT70 > 50 days, SOMO10 > 24 mg m^{-3} day) grows from 15.4 % (11.8 %, 11.0 %, 32.0 %) in 2013–2016 to 55.7 % (45.6 %, 39.3 %, 67.8 %) in 2017–2019.

3.1.2. Ozone-related mortality based on TAP database

We use premature respiratory mortalities attributable to long-term O_3 exposure (denoted as O_3-mortality) to more intuitively exhibit the health impacts of O_3 exposure. Fig. 3(a–b) show spatial distributions of 7-year mean and trend in O_3-mortality during 2013–2019 over China; Fig. 3(c–d) present age-specific O_3-mortality and the corresponding trend in 31 provinces of China. The population-weighted AVGMDA8 and the corresponding trend in each province are also shown. High O_3-mortalities are distributed over North China Plain, Yangtze River Delta, Pearl River Delta, and Sichuan Basin, where O_3 levels (Fig. 2(a1)) and population densities exhibit high values; top five provinces with >10 thousand O_3-mortalities are Shandong, Henan, Guangdong, Jiangsu, and Hebei. Increasing trends in O_3-mortalities are observed across almost the whole China, with hotspots located in developed cities; top five provinces with O_3-mortality trends over 1.0 thousand

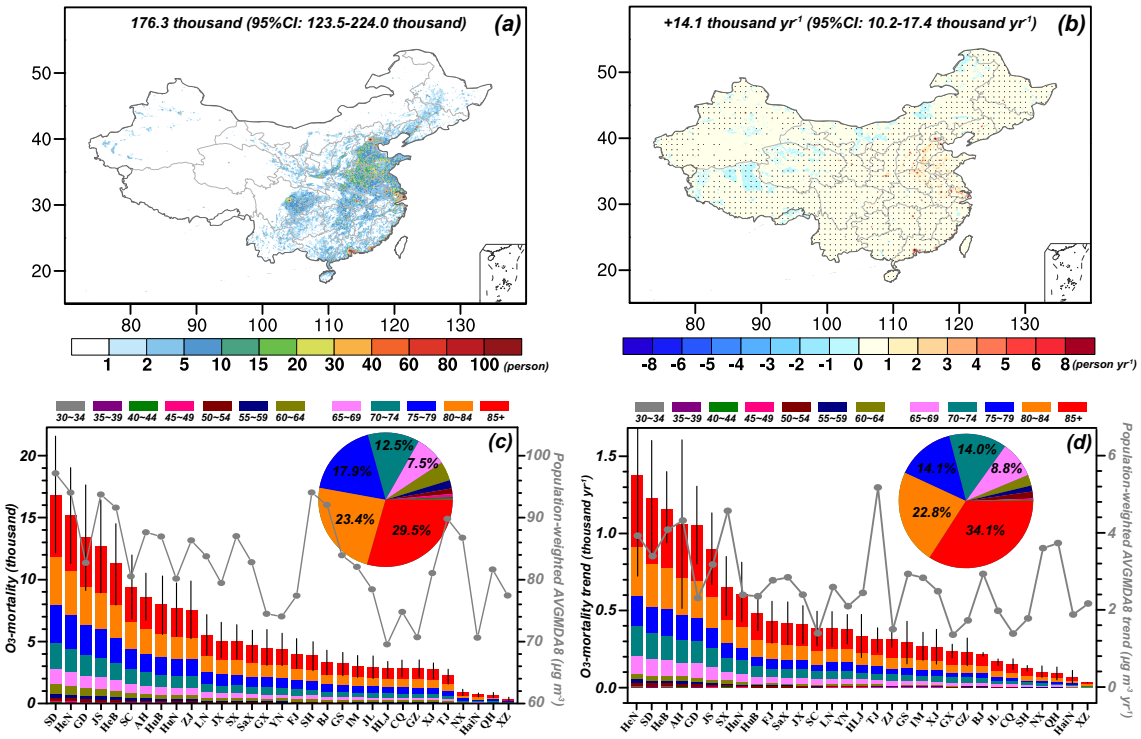

Fig. 3. Spatial distributions of 7-year (a) mean and (b) trend in premature respiratory mortalities attributable to long-term O_3 exposure (denoted as O_3-mortality) during 2013–2019 over China. Age-specific (c) O_3-mortality and (d) corresponding trend in 31 provinces of China. Statistically significant trends with 95 % confidence level are marked with dots in (b). The pie charts in (c) and (d) exhibit percentage contributions from different age groups. The dot lines in (c) and (d) are population-weighted AVGMDA8 and the corresponding trend in each province. The error bars in (c) and (d) show the 95 % confidence interval (CI). The provinces that the abbreviations represent in (c) and (d) are listed in Table 2.

yr^{-1} are Henan, Shandong, Hebei, Anhui, and Guangdong. Rapid O_3 increases (maximum O_3 trend of $+6.0$ μg m^{-3} yr^{-1}, Fig. 2(a2)) contribute greatly to the increasing O_3-mortality trends in Anhui. Analyzing the severities of ozone-related mortalities in all the provinces in China, population-weighted AVGMDA8 concentrations show different patterns with large values in some provinces where the calculated O_3-mortality is weak (e.g., Shanghai and Tianjin). This is because, in these provinces, the O_3 pollution is serious but the population base is small. All these can indicate that the results generated from population-weighted estimates may not be suitable for accurately assessing premature mortality.

The national annual O_3-mortality is estimated to increase by 51.0 % from 2013 to 2019, which is quite close to that in Xiao et al. (2022) who reported an increase of 49.3 %. For both O_3-mortality value and trend, the elder groups contribute more. The national O_3-mortality is 176.3 thousand (95 % CI: 123.5–224.0 thousand) with an increasing trend of 14.1 thousand yr^{-1} (95 % CI: 10.2–17.4 thousand yr^{-1}) during 2013–2019; the elderly over 65 years old contribute 90.8 % and 93.8 % of the total O_3-mortality and its increasing trend, which can be explained by the high baseline mortality rates for the elderly over 65 (Fig. 5(b)).

3.1.3. Comparisons between TAP-based ozone-related mortality with others

Since the availability of CNEMC O_3 measurements, the O_3-mortality estimation has been widely based on the CNEMC O_3 concentrations. However, the urban-site-dominant O_3 observations which almost can only stand for urban pollution levels may cause possible deviations when assessing O_3-mortality at a national or provincial level, as introduced in

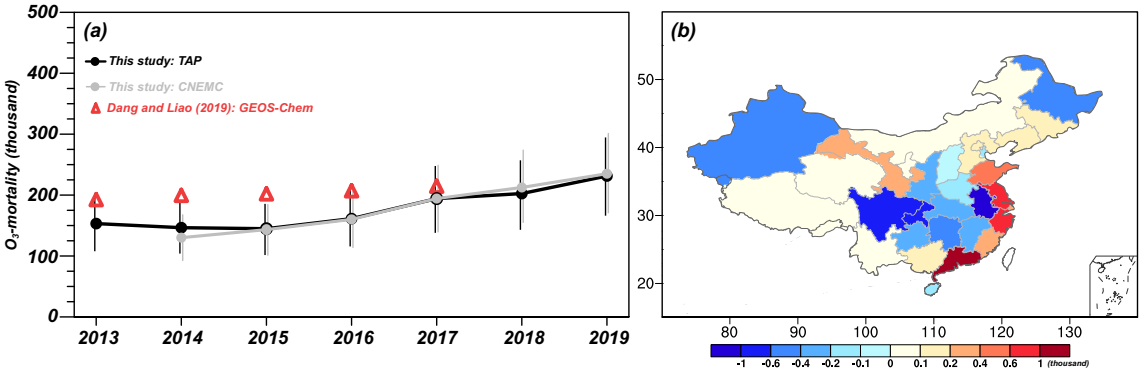

Fig. 4. (a) Yearly national premature respiratory mortalities attributable to long-term O_3 exposure (denoted as O_3-mortality) during 2013–2019 for China based on TAP grid vs. CNEMC site O_3 concentrations. (b) Differences between provincial CNEMC and TAP (CNEMC minus TAP) O_3-mortalities over China averaged during 2014–2019. The CNEMC O_3-mortality for year 2013 in (a) is not shown due to the unavailability of partial CNEMC O_3 concentrations in 2013. Also shown in (a) is yearly national O_3-mortality based on chemical transport model GEOS-Chem collected from previous literature. The error bars in (a) indicate the 95 % confidence interval (CI). The calculated CNEMC O_3-mortality, TAP O_3-mortality, as well as their difference for each province in (b) are listed in Table 2.

Introduction section. Here, we conduct comparisons of national (provincial) O_3-mortality based on TAP grid vs. CNEMC site O_3 concentrations in Fig. 4 and Table 2. Given that TAP O_3 database not only reproduces the observed O_3 concentrations fairly well (Section 2.1) but also shows advantage in spatiotemporal coverage, the TAP-based O_3-mortality is taken as a credible standard here. The TAP-based national (provincial) O_3-mortality is the sum of all gridded O_3-mortalities over the whole China (this province). The CNEMC-based provincial O_3-mortality is calculated by using the provincial population data and the O_3 concentration averaged over all CNEMC sites in this province; the CNEMC-based national O_3-mortality is the sum of all CNEMC-based provincial O_3-mortalities.

As shown in Fig. 4(a), the national O_3-mortality based on CNEMC O_3 concentrations is quite close to that based on TAP O_3 concentrations for each year; the CNEMC (TAP) national annual O_3-mortality averaged during 2014–2019 is calculated to be 179.2 thousand (95%CI: 125.2–226.5 thousand) (180.1 thousand, 95%CI: 126.36–228.7 thousand). Although estimating the national O_3-mortality using CNEMC site O_3 concentrations is practicable, large bias exists in estimating provincial O_3-mortalities. Compared with TAP-based provincial O_3-mortalities, CNEMC-based O_3-mortalities are overestimated in coastal provinces with the largest positive deviation of +1.3 thousand in Guangdong, but underestimated in most provinces located in central China with the largest negative deviation of −1.4 thousand in Anhui (Fig. 4(b) and Table 2).

We also conduct comparisons with national annual O_3-mortality based on chemical transport model taken from previous literature. Dang and Liao (2019), who applied GEOS-Chem model to investigate O_3-related health impacts, exhibited higher O_3-mortality than TAP-based O_3-mortality (Fig. 4(a)). The national O_3-mortality averaged over 2013–2017 is estimated to be 209.2 thousand and 176.2 thousand (95%CI: 111.8–204.0 thousand) for GEOS-Chem and TAP, respectively. The differences arise from O_3 concentration estimates and relative risk estimates. The summer O_3 concentrations simulated by GEOS-Chem are vastly overestimated with NMB of +35.8 %; the relative risk estimate in Dang and Liao (2019) uses warm-season 1-h daily maximum O_3 (MDA1 O_3) concentration and corresponding threshold concentration as well as β value which were derived from Jerrett et al. (2009), rather than annual mean MDA8 O_3 concentration used in this study which refers to Turner et al. (2016).

Table 2
Provincial-level O_3-mortality averaged during 2014–2019 derived from CNEMC vs. TAP O_3 concentrations.

Province		CNEMC (thousand, 95%CI)	TAP (thousand, 95%CI)	MB[a] (thousand)	NMB[b] (%)
Beijing	BJ	3.56 (2.46, 4.42)	3.43 (2.42, 4.34)	+0.12	+3.6
Tianjin	TJ	2.21 (1.53, 2.75)	2.35 (1.65, 2.97)	−0.14	−5.9
Hebei	HeB	11.87 (8.35, 14.98)	11.74 (8.27, 14.83)	+0.13	+1.1
Shanxi	SX	5.06 (3.55, 6.35)	5.15 (3.62, 6.52)	−0.09	−1.7
Neimenggu	IM	3.19 (2.25, 4.09)	3.11 (2.18, 3.96)	+0.08	+2.7
Liaoning	LN	5.93 (4.19, 7.60)	5.74 (4.02, 7.29)	+0.19	+3.3
Jilin	JL	3.2 (2.23, 4.09)	3.06 (2.13, 3.91)	+0.14	+4.5
Heilongjiang	HLJ	2.53 (1.76, 3.29)	3.04 (2.11, 3.91)	−0.51	−16.7
Shanghai	SH	4.22 (2.98, 5.31)	3.94 (2.78, 4.98)	+0.28	+7.2
Jiangsu	JS	13.79 (9.67, 17.26)	13.11 (9.25, 16.56)	+0.68	+5.2
Zhejiang	ZJ	8.25 (5.71, 10.34)	7.64 (5.36, 9.71)	+0.61	+8.0
Anhui	AH	7.31 (5.14, 9.23)	8.73 (6.14, 11.04)	−1.42	−16.3
Fujian	FJ	4.34 (3.01, 5.50)	4.13 (2.88, 5.28)	+0.21	+5.2
Jiangxi	JX	4.79 (3.29, 6.03)	5.07 (3.54, 6.48)	−0.28	−5.5
Shandong	SD	17.95 (12.7, 22.57)	17.41 (12.32, 21.93)	+0.54	+3.1
Henan	HeN	15.4 (10.81, 19.31)	15.52 (10.96, 19.58)	−0.12	−0.7
Hubei	HuB	7.76 (5.40, 9.81)	7.97 (5.59, 10.12)	−0.21	−2.7
Hunan	HuN	7.3 (5.06, 9.27)	7.72 (5.39, 9.86)	−0.42	−5.5
Guangdong	GD	14.99 (10.49, 19.03)	13.69 (9.57, 17.43)	+1.30	+9.5
Guangxi	GX	4.68 (3.24, 5.98)	4.51 (3.13, 5.79)	+0.16	+3.6
Hainan	HaiN	0.6 (0.41, 0.77)	0.74 (0.51, 0.95)	−0.14	−19.1
Chongqing	CQ	2.1 (1.41, 2.63)	2.79 (1.94, 3.58)	−0.69	−24.6
Sichuan	SC	8.57 (5.93, 10.92)	9.22 (6.43, 11.78)	−0.65	−7.1
Guizhou	GZ	2.49 (1.70, 3.18)	2.84 (1.96, 3.65)	−0.34	−12.1
Yunnan	YN	4.47 (3.09, 5.71)	4.44 (3.08, 5.69)	+0.04	+0.8
Xizang	XZ	0.46 (0.32, 0.59)	0.36 (0.25, 0.47)	+0.09	+25.4
Shaanxi	SaX	4.48 (3.13, 5.70)	4.73 (3.31, 6.02)	−0.25	−5.3
Gansu	GS	3.67 (2.57, 4.64)	3.4 (2.38, 4.33)	+0.26	+7.7
Qinghai	QH	0.77 (0.54, 0.97)	0.74 (0.52, 0.94)	+0.03	+4.2
Ningxia	NX	0.96 (0.68, 1.22)	0.95 (0.67, 1.2)	+0.02	+1.8
Xinjiang	XJ	2.34 (1.62, 2.98)	2.86 (2.00, 3.64)	−0.52	−18.2

[a] MB (mean bias) = CNEMC − TAP.
[b] NMB (normalized mean bias) = (CNEMC − TAP)/TAP × 100%.

3.2. Effects of individual factors on ozone-related mortality rises during 2013–2019

We investigate the cause for O_3-mortality rises during 2013–2019 by quantifying the respective contribution of each factor, i.e., baseline mortality rate (BMR), population (Pop), age structure (AgeStru), and O_3 concentration (Conc). Fig. 5(c) shows yearly national O_3-mortality during 2013–2019 in normal-condition experiment and four sensitivity experiments. When all factors vary from 2013 to 2019, the national O_3-mortality exhibits an increasing trend of +14.1 thousand yr^{-1} (95 % CI: 10.2–17.4 thousand yr^{-1}); the results from four sensitivity experiments show that the national O_3-mortality varies at a rate of +12.7 thousand yr^{-1} (95 % CI: 9.2–15.6 thousand yr^{-1}), +5.8 thousand yr^{-1} (95 % CI: 4.0–7.4 thousand yr^{-1}), +1.0 thousand yr^{-1} (95 % CI: 0.7–1.2 thousand yr^{-1}), −5.4 thousand yr^{-1} (95 % CI: −6.9 to −3.7 thousand yr^{-1}), owing to changes in Conc alone, AgeStru alone, Pop alone, BMR alone, respectively. The deterioration of O_3 air quality, shown as significant increase in O_3 concentrations (Fig. 2(a2)), is regarded as the leading factor which contributes 90.1 % of national O_3-mortality rise during 2013–2019. The spatial distribution of leading factor which most influences O_3-mortality trend over China (Fig. 5(d)) also shows that O_3 concentration variation dominates O_3-mortality trend over most regions of China (84.2 % of China's territorial area excluding regions without population).

As shown in Fig. 5(a), the proportion of the elderly over 65 years old in total population (adults above 30) has increased from 16.0 % in 2013 to 19.3 % in 2019. The change in age structure, which specifically means the aggravation of population aging here, is the second most important factor which leads to O_3-mortality rise. Compared with the change in age structure, national population growth plays a minor role in O_3-mortality rise; the increase of 11.4 % in national population results in a national O_3-mortality trend of +1.0 thousand yr^{-1} (95 % CI: 0.7–1.2 thousand yr^{-1}). Opposite to above three factors, the decreased baseline mortality rate (Fig. 5(b)) owing to improved medical conditions brings about positive health impacts and leads to a negative O_3-mortality trend of −5.4 thousand yr^{-1} (95 % CI: −6.9 to −3.7 thousand yr^{-1}).

3.3. Effects of individual factors on ozone-related mortality rises from 2019 to 2030 under SSPs

Future changes in annual O_3-mortality from 2019 to 2030 under three SSP scenarios are projected in Fig. 6. SSPs combine pathways of socioeconomic development with targets to achieve a certain level of climate mitigation. SSP1-2.6 represents the sustainability pathway which leads to improvements in both air quality and climate. SSP2-4.5 represents the medium part of the range of future forcing pathways, and is the updated version of the RCP4.5 scenario in CMIP5. SSP5-8.5 represents the high-fossil-fuel-development pathway which produces anthropogenic radiative forcing of 8.5 W m^{-2} in 2100.

As shown in Fig. 6(d), O_3-mortality rises are predicted for all three scenarios; the national O_3-mortality is projected to increase by 50.4 thousand (95 % CI: 37.8–63.0 thousand) in SSP1-2.6, 87.4 thousand (95 % CI: 65.5–109.2 thousand) in SSP2-4.5, and 103.7 thousand (95 % CI: 77.8–129.6 thousand) in SSP5-8.5, respectively. Four underlying causes, i.e., BMR, Pop, AgeStru, and Conc, make distinct contributions to future O_3-mortality rises. Among the four factors, age structure change contributes most to O_3-mortality rises. From 2019 to 2030, the proportion of the young and middle-aged below 50 years old in total population (for adults above 30) will decline from 48.5 % in 2019 to 40.7 % in 2030 while that of the elderly over 70 years old will increase from 11.6 % in 2019 to 17.8 % in

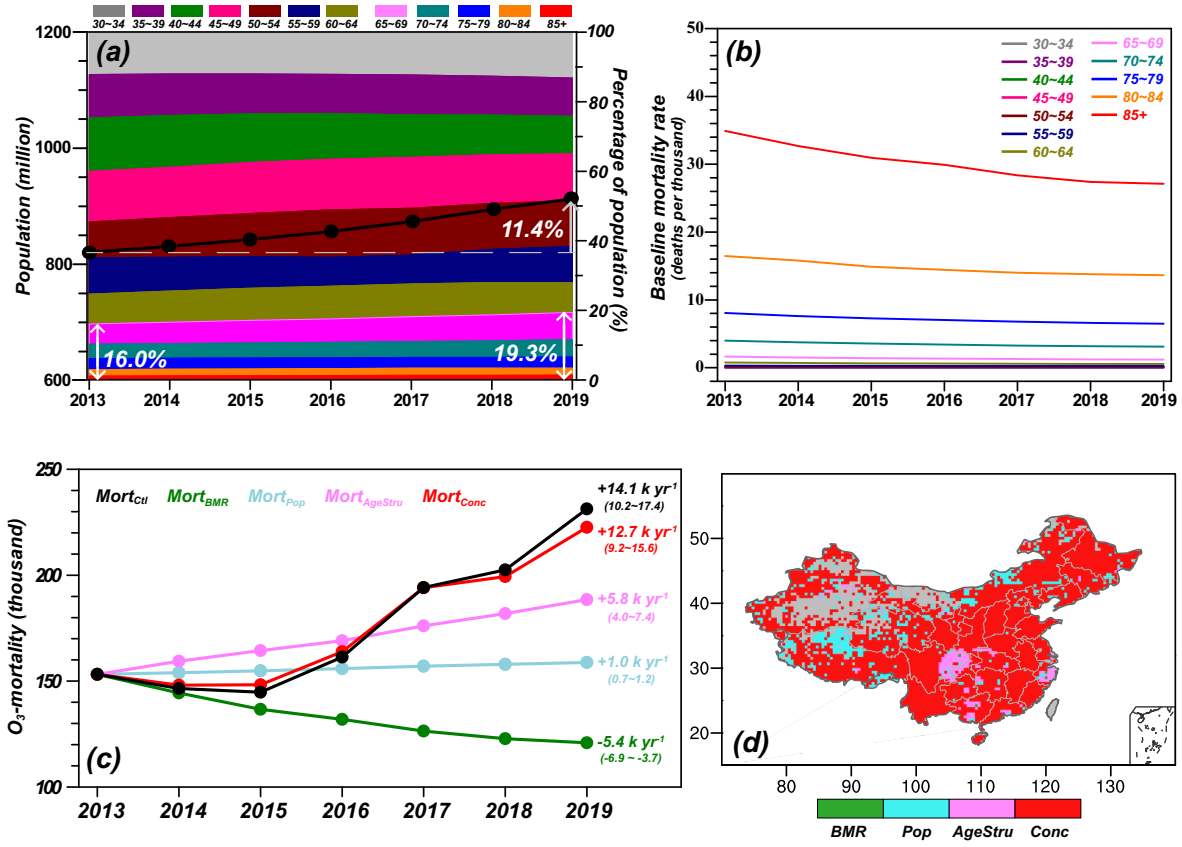

Fig. 5. (a) National population for adults above 30 (black dotted line) and age structure (colored stacked chart) during 2013–2019 for China. (b) China's age-specific baseline mortality rates of chronic respiratory disease during 2013–2019. (c) Yearly national premature respiratory mortalities attributable to long-term O_3 exposure (denoted as O_3-mortality) during 2013–2019 in normal-condition experiment and four sensitivity experiments. (d) Spatial distribution of leading factor which most influences 7-year trend in O_3-mortality. The percentage of increase in national population from 2013 to 2019 and the proportions of population for the elderly over 65 years old in 2013 and 2019 are listed in white values in (a). The calculated 7-year trend in national O_3-mortality in each experiment is presented in colored value in (c). The values in brackets mean 95 % confidence interval (CI). Grey areas (except Taiwan) are regions with no population in (d).

2030 (Fig. 6(a)). This change in age structure, i.e., population aging, will result in significant O_3-mortality rises of 137.9–160.5 thousand among three scenarios. By contrast, population growth of 74.1 million (Fig. 6(a)) has a slight effect; the O_3-mortality will increase by only 6.7–7.8 thousand owing to the change in population size alone. Due to improving medical conditions, the BMR in 2030 for the young and middle-aged below 70 years old will change little (relative to year 2019) but that for the elderly above 70 will decrease a lot (-22.6 deaths/10 thousand, Fig. 6(b)), which will bring about beneficial health outcomes and lead to O_3-mortality declines of 85.9–99.9 thousand. Fig. 6(c) exhibits future changes in O_3 concentrations in 2030 relative to 2019 under three SSP scenarios, which are obtained from four individual CMIP6 models. The multi-model ensemble mean MDA8 O_3 concentration will change by -8.1 μg m^{-3} in SSP1-2.6, $+2.4$ μg m^{-3} in SSP2-4.5, and $+4.6$ μg m^{-3} in SSP5-8.5, respectively. The radically different changes in O_3 concentrations will cause different O_3-mortality changes, ranging from -8.3 thousand (95 % CI: -6.2 to -10.4 thousand) in SSP1-2.6 to $+35.3$ thousand (95 % CI: 26.5–44.2 thousand) in SSP5-8.5.

During the past seven years (2013–2019), rapid O_3 concentration increase ($+2.5$ μg m^{-3} yr^{-1} at the national level) has been the primary factor which leads to O_3-mortality rises. However, O_3 concentrations are projected to increase at a lower rate ($+0.4$ μg m^{-3} yr^{-1} in SSP5-8.5) or even decrease (-0.7 μg m^{-3} yr^{-1} in SSP1-2.6) in the coming decade (2019–2030). In fact, a latest research has reported that summertime surface O_3 over eastern China decreased by 5.5 ppbv in 2020 compared to the 2019 level, representing an unprecedented ozone reduction since 2013 (Yin et al., 2021). Therefore, persistent population aging will take place of the deterioration of O_3 air quality and become the leading factor causing future O_3-mortality rises in the coming decade, also suggesting an urgent need to take more stringent (than currently planned) emission reduction measures to offset the adverse effects caused by population aging in the near future.

4. Conclusions and discussion

Based on gridded O_3 concentration provided by a newly developed database named TAP and generated by a data-fusion algorithm that combines in situ observations, satellite remote sensing measurements and model simulations, this study examines the spatiotemporal characteristics of O_3-related health impacts in China during 2013–2019 and quantifies the relative contributions of four underlying driving factors (population size, population age structure, mortality rate for respiratory disease, and O_3 concentration) to the changes in premature respiratory mortalities attributable to long-term O_3 exposure (O_3-mortality) in China. By using gridded O_3 concentration projected by CMIP6 models, we also predict future (2019–2030) changes in O_3-mortality under different SSP scenarios and distinguish the respective contribution of each factor.

Four ozone-health-related metrics, i.e., AVGMDA8, 4MDA8, NDGT70, and SOMO10 all exhibit the maximum values over North China Plain. Increasing trends of four metrics from 2013 to 2019 are observed across almost the whole China; the maximum values of seven-year trends are also located over North China Plain for all four metrics. The O_3-mortality is used to more intuitively exhibit the health impacts of O_3 exposure. The national annual O_3-mortality is 176.3 thousand (95 % CI: 123.5–224.0 thousand) averaged during 2013–2019 with an increasing trend of 14.1 thousand yr^{-1} (95 % CI: 10.2–17.4 thousand yr^{-1}); the elderly over 65 years old

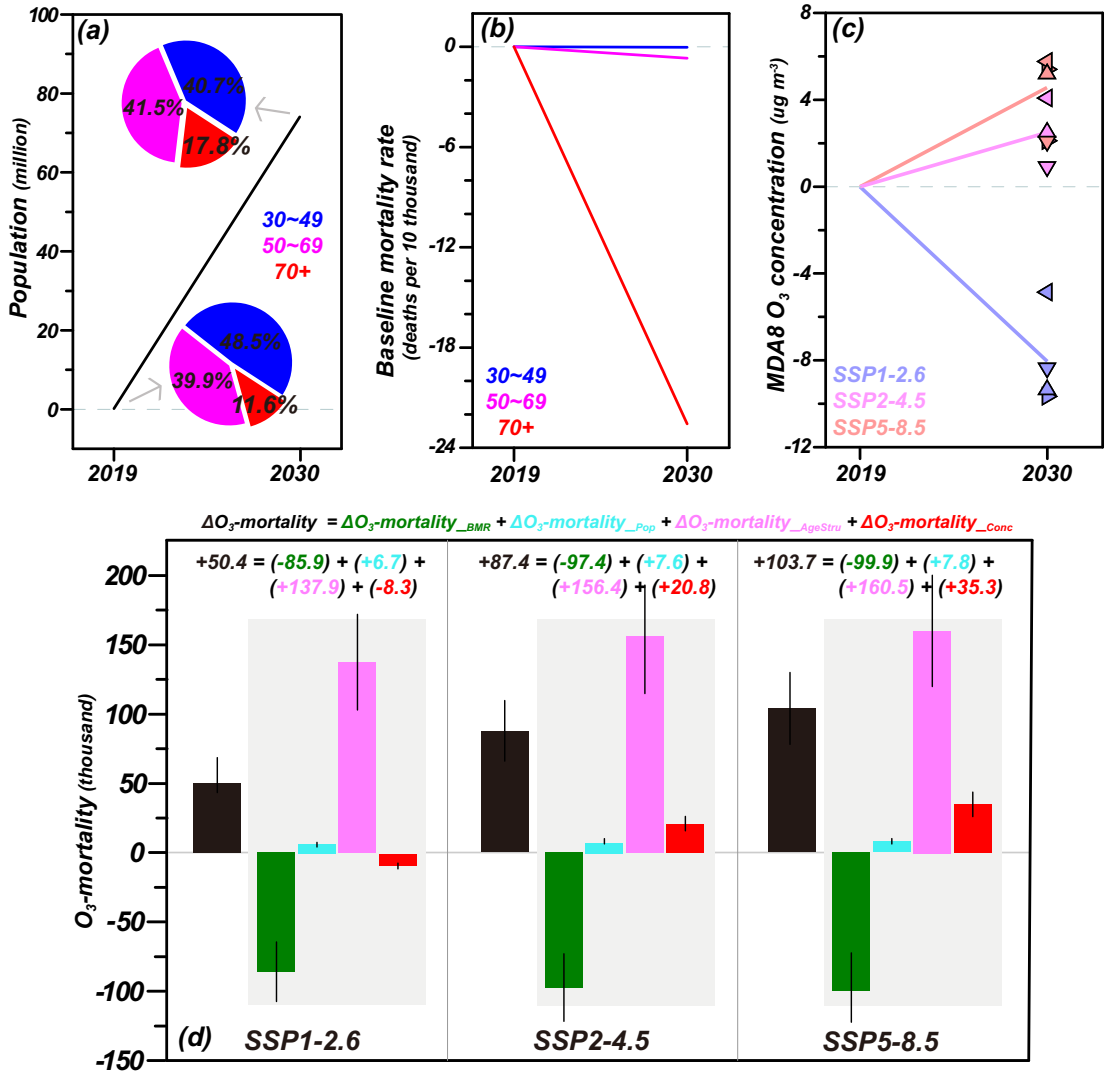

Fig. 6. Future changes in (a) national population (Pop) and age structure (AgeStru) for adults above 30, (b) baseline mortality rate (BMR), (c) O_3 concentration (Conc), (d) national premature respiratory mortalities attributable to long-term O_3 exposure (O_3-mortality) in 2030 relative to 2019. The two pie charts in (a) exhibit population percentage for three age groups in 2019 and 2030. Future changes in O_3 concentration in (c) and O_3-mortality in (d) are presented under three SSP scenarios. Triangles represent results from four individual CMIP6 models and lines represent multi-model ensemble means in (c). The multi-model ensemble mean O_3-mortality change and contributions from four factors are exhibited in colored bars in (d). The error bars in (d) indicate the 95 % confidence interval (CI).

contribute 90.8 % and 93.8 % of the total O_3-mortality and its increasing trend, respectively. Top five provinces with O_3-mortality trends over 1.0 thousand yr^{-1} are Henan, Shandong, Hebei, Anhui, and Guangdong.

We also conduct comparisons of national (provincial) O_3-mortality based on TAP vs. CNEMC O_3 concentrations. The national O_3-mortality based on CNEMC site O_3 concentrations is quite close to that based on TAP grid O_3 concentrations for each year. However, compared with TAP-based provincial O_3-mortalities, CNEMC-based O_3-mortalities are overestimated in coastal provinces with the largest positive deviation of +1.3 thousand in Guangdong, but underestimated in most provinces located in central China with the largest negative deviation of −1.4 thousand in Anhui.

Sensitivity experiments conducted during 2013–2019 show that the change in O_3 concentration alone, population age structure alone, population size alone, mortality rate for respiratory disease alone leads to national O_3-mortality trend of +12.7 thousand yr^{-1} (95 % CI: 9.2–15.6 thousand yr^{-1}), +5.8 thousand yr^{-1} (95 % CI: 4.0–7.4 thousand yr^{-1}), +1.0 thousand yr^{-1} (95 % CI: 0.7–1.2 thousand yr^{-1}), −5.4 thousand yr^{-1} (95 % CI: −6.9 to −3.7 thousand yr^{-1}), respectively. The significant increase in O_3 concentration is regarded as the leading factor, which contributes 90.1 % of national O_3-mortality rise (+14.1 thousand yr^{-1} (95 % CI: 10.2–17.4 thousand yr^{-1})) during 2013–2019.

Future changes in O_3-mortality are also examined from 2019 to 2030. The national O_3-mortality is projected to increase by 50.4 thousand (95 % CI: 37.8–63.0 thousand) in SSP1-2.6, 87.4 thousand (95 % CI: 65.5–109.2 thousand) in SSP2-4.5, and 103.7 thousand (95 % CI: 77.8–129.6 thousand) in SSP5-8.5, respectively. Among four underlying factors, age structure change contributes most to O_3-mortality rises. The proportion of the elderly over 70 years old in total population (for adults above 30) will increase from 11.6 % in 2019 to 17.8 % in 2030. This change in age structure, i.e., population aging, will result in significant O_3-mortality rises of 137.9–160.5 thousand. It is noted that rapid O_3 concentration increase of +2.5 μg m^{-3} yr^{-1} at the national level is the primary factor for 2013–2019 O_3-mortality rises. However, from 2019 to 2030, O_3 concentrations are projected to increase at a lower rate (+0.4 μg m^{-3} yr^{-1} in SSP5-8.5) or even decrease (−0.7 μg m^{-3} yr^{-1} in SSP1-2.6). For the coming decade, population aging, instead of O_3 concentration increase, will become the leading cause of future O_3-mortality rises.

There are some limitations in our manuscript, which could be improved in future studies. CMIP6 projections are designed before 2016 (Eyring et al.,

2016). Therefore, all future scenarios did not take Coronavirus Disease 2019 (COVID-19) effect into account. A recent study modified emissions scenario projections to account for the effects of COVID-19 (Lamboll et al., 2021). The updated emission projection can be used to predict future ozone level and associated mortalities in future studies. In addition, we mainly focus on the ozone-related mortality at the national level in this study. But the observations have shown different changes in ozone concentrations in urban/suburban (e.g., increase) and rural (e.g., decrease) areas due to emission-control measures implemented by the government (Liu and Wang, 2020; Wang et al., 2022; Zhang et al., 2022). The different changing patterns of ozone concentrations, including human migration from the countryside to urban cities, will cause significantly different results for ozone-related disease burdens in urban/suburban and rural areas in recent decades (Chen et al., 2018; Malashock et al., 2022). In order to quantitatively analyze the urban/suburban and rural health impacts attributable to ozone exposure and the relative contributions of four underlying driving factors (i.e., population size, population age structure, mortality rate for respiratory disease, and O_3 concentration), a finer resolution of gridded ozone database (e.g., 1 km) should be developed and used in future studies. All the results about the ozone-related mortalities in urban/suburban and rural areas and the major driving factor will be detailedly discussed, which may be helpful to make future environmental and public health policies.

CRediT authorship contribution statement

Lei Chen: Conceptualization, Methodology, Writing – original draft, Formal analysis, Funding acquisition. **Hong Liao:** Resources, Writing – review & editing, Supervision, Funding acquisition. **Jia Zhu:** Conceptualization, Methodology, Writing – review & editing, Formal analysis, Funding acquisition. **Ke Li:** Validation, Writing – review & editing. **Yang Bai:** Investigation, Visualization. **Xu Yue:** Validation, Writing – review & editing. **Yang Yang:** Resources, Visualization. **Jianlin Hu:** Resources, Investigation. **Meigen Zhang:** Validation, Writing – review & editing.

Data availability

The TAP O_3 database can be publicly accessed from http://tapdata.org.cn/. The observed O_3 concentrations from CNEMC can be obtained at http://106.37.208.233:20035/. The future ozone concentrations taken from CIMP6 models are downloaded from https://pcmdi.llnl.gov/CMIP6/. The gridded population data are from LandScan (https://landscan.ornl.gov/). The China Statistical Yearbook (http://www.stats.gov.cn/tjsj/ndsj/) provides provincial population. The future national-level population and age structure data are from Population Pyramid (https://www.populationpyramid.net/china/2030/). The historical baseline mortality rates are obtained from Global Health Data Exchange (http://ghdx.healthdata.org/gbd-results-tool), and the future predicted mortality rates are from WHO Global Health Estimates (https://colinmathers.com/2022/05/10/projections-of-global-deaths-from-2016-to-2060/).

Declaration of competing interest

The authors declare that they have no known competing financial interests or personal relationships that could have appeared to influence the work reported in this paper.

Acknowledgements

This work was supported by National Natural Science Foundation of China (42007195), University Natural Science Research Foundation of Jiangsu Province (21KJB170004), Carbon Peak Carbon Neutral Science and Technology Innovation Foundation of Jiangsu Province (BK20220031), State Key Laboratory of Atmospheric Boundary Layer Physics and Atmospheric Chemistry (LAPC-KF-2022-05), State Environmental Protection Key Laboratory of Sources and Control of Air Pollution Complex (SCAPC202114), and National Key R&D Program of China (2019YFA0606804).

References

Anenberg, S.C., Horowitz, L.W., Tong, D.Q., West, J.J., 2010. An estimate of the global burden of anthropogenic ozone and fine particulate matter on premature human mortality using atmospheric modeling. Environ. Health Perspect. 118, 1189–1195. https://doi.org/10.1289/ehp.0901220.

Chen, K., Fiore, A.M., Chen, R., Jiang, L., Jones, B., Schneider, A., Peters, A., Bi, J., Kan, H., Kinney, P.L., 2018. Future ozone-related acute excess mortality under climate and population change scenarios in China: a modeling study. PLoS Med. 15 (7), e1002595. https://doi.org/10.1371/journal.pmed.1002598.

Chen, G., Xiang, H., Mao, Z., Huo, W., Guo, Y., Wang, C., Li, S., 2019. Is long-term exposure to air pollution associated with poor sleep quality in rural China? Environ. Int. 133, 105205. https://doi.org/10.1016/j.envint.2019.105205.

Chen, L., Zhu, J., Liao, H., Yang, Y., Yue, X., 2020. Meteorological influences on PM2.5 and O3 trends and associated health burden since China's clean air actions. Sci. Total Environ. 744, 140837. https://doi.org/10.1016/j.scitotenv.2020.140837.

Chen, K.Y., Wang, P.F., Zhao, H., Wang, P., Gao, A.F., Myllyvirta, L., Zhang, H.L., 2021. Summertime O3 and related health risks in the North China plain: a modeling study using two anthropogenic emission inventories. Atmos. Environ. 246, 118087. https://doi.org/10.1016/j.atmosenv.2020.118087.

China's National Bureau of Statistics 2020, 2020. China Statistical Yearbook. http://www.stats.gov.cn/tjsj/ndsj/2020/indexeh.htm.

Cohen, A.J., Brauer, M., Burnett, R., Anderson, H.R., Frostad, J., Estep, K., Balakrishnan, K., Brunekreef, B., Dandona, L., Dandona, R., Feigin, V., Freedman, G., Hubbell, B., Jobling, A., Kan, H., Knibbs, L., Liu, Y., Martin, R., Morawska, L., Pope III, C.A., Shin, H., Straif, K., Shaddick, G., Thomas, M., van Dingenen, R., van Donkelaar, A., Vos, T., Murray, C.J.L., Forouzanfar, M.H., 2017. Estimates and 25-year trends of the global burden of disease attributable to ambient air pollution: an analysis of data from the global burden of diseases study 2015. Lancet 389 (10082), 1907–1918. https://doi.org/10.1016/S0140-6736(17)30505-6.

Dang, R., Liao, H., 2019. Radiative forcing and health impact of aerosols and ozone in China as the consequence of clean air actions over 2012–2017. Geophys. Res. Lett. 46 (21), 12511–12519. https://doi.org/10.1029/2019GL084605.

Ding, D., Xing, J., Wang, S., Liu, K., Hao, J., 2019. Estimated contributions of emissions controls, meteorological factors, population growth, and changes in baseline mortality to reductions in ambient PM2.5 and PM2.5-related mortality in China, 2013–2017. Environ. Health Perspect. 127 (6), 067009. https://doi.org/10.1289/EHP4157.

Eyring, V., Bony, S., Meehl, G.A., Senior, C.A., Stevens, B., Stouffer, R.J., Taylor, K.E., 2016. Overview of the coupled model intercomparison project phase 6 (CMIP6) experimental design and organization. Geosci. Model Dev. 9, 1937–1958. https://doi.org/10.5194/gmd-9-1937-2016.

Feng, Z.Z., De Marco, A., Anav, A., Gualtieri, M., Sicard, P., Tian, H., Fornasier, F., Tao, F., Guo, A., Paoletti, E., 2019. Economic losses due to ozone impacts on human health, forest productivity and crop yield across China. Environ. Int. 131, 104966. https://doi.org/10.1016/j.envint.2019.104966.

Fleming, L.Z., Doherty, R.M., Schneidemesser, E.von, Malley, C.S., Cooper, O.R., Pinto, J.P., Colette, A., Xu, X.B., Simpson, D., Schultz, M.G., Lefohn, A.S., Hamad, S., Moolla, R., Solberg, S., Feng, Z.Z., 2018. Tropospheric Ozone Assessment Report: Present-day ozone distribution and trends relevant to human health. Elementa (Wash. D.C.) 6, 12. https://doi.org/10.1525/elementa.273.

Gao, L., Yue, X., Meng, X., Du, L., Lei, Y., Tian, C., Qiu, L., 2020. Comparison of ozone and PM2.5 concentrations over urban, suburban, and background sites in China. Adv. Atmos. Sci. 37, 1297–1309. https://doi.org/10.1007/s00376-020-0054-2.

Geng, G.N., Zheng, Y.X., Zhang, Q., Xue, T., Zhao, H.Y., Tong, D., Zheng, B., Li, M., Liu, F., Hong, C.P., He, K.B., Davis, S.J., 2021. Drivers of PM2.5 air pollution deaths in China 2002–2017. Nat. Geosci. 14 (9), 645–650. https://doi.org/10.1038/s41561-021-00792-3.

Gidden, M.J., Riahi, K., Smith, S.J., Fujimori, S., Luderer, G., Kriegler, E., van Vuuren, D.P., van den Berg, M., Feng, L., Klein, D., Calvin, K., Doelman, J.C., Frank, S., Fricko, O., Harmsen, M., Hasegawa, T., Havlik, P., Hilaire, J., Hoesly, R., Horing, J., Popp, A., Stehfest, E., Takahashi, K., 2019. Global emissions pathways under different socioeconomic scenarios for use in CMIP6: a dataset of harmonized emissions trajectories through the end of the century. Geosci. Model Dev. 12 (4), 1443–1475. https://doi.org/10.5194/gmd-12-1443-2019.

Guo, Y., Jiang, Y.D., Huang, B.Z., Xing, J.J., Wei, Z.Z., 2021. Health impact of PM2.5 and O3 and forecasts for next 10 years in China. Res. Environ. Sci. 34 (4), 1023–1032. https://doi.org/10.13198/j.issn.1001-6929.2020.12.03.

Jerrett, M., Burnett, R.T., Pope, C.A., Ito, K., Thurston, G., Krewski, D., Shi, Y., Calle, E., Thun, M., 2009. Long-term ozone exposure and mortality. N. Engl. J. Med. 360 (11), 1085–1095. https://doi.org/10.1056/NEJMoa0803894.

Jiang, Z., Jolleys, M.D., Fu, T.M., Palmer, P.I., Ma, Y., Tian, H., Li, J., Yang, X., 2020. Spatiotemporal and probability variations of surface PM2.5 over China between 2013 and 2019 and the associated changes in health risks: an integrative observation and model analysis. Sci. Total Environ. 723, 137896. https://doi.org/10.1016/j.scitotenv.2020.137896.

Kong, L., Tang, X., Zhu, J., Wang, Z.F., Li, J.J., Wu, H.J., Wu, Q.Z., Chen, H.S., Zhu, L.L., Wang, W., Liu, B., Wang, Q., Chen, D.H., Pan, Y.P., Song, T., Li, F., Zheng, H.T., Jia, G.L., Lu, M.M., Wu, L., Carmichael, G.R., 2021. A 6-year-long (2013–2018) high-resolution air quality reanalysis dataset in China based on the assimilation of surface observations from CNEMC. Earth Syst. Sci. Data 13, 529–570. https://doi.org/10.5194/essd-13-529-2021.

Lamboll, R.D., Jones, C.D., Skeie, R.B., Fiedler, S., Samset, B.H., Gillett, N.P., Rogelj, J., Forster, P.M., 2021. Modifying emissions scenario projections to account for the effects of COVID-19: protocol for CovidMIP. Geosci. Model Dev. 14, 3683–3695. https://doi.org/10.5194/gmd-14-3683-2021.

Lefohn, A.S., Malley, C.S., Smith, L., Wells, B., Hazucha, M., Simon, H., Naik, V., Mills, G., Schultz, M.G., Paoletti, E., Marco, A.D., Xu, X.B., Zhang, L., Wang, T., Neufeld, H.S., Musselman, R.C., Tarasick, D., Brauer, M., Feng, Z.Z., Tang, H.Y., Kobayashi, K., Sicard, P., Solberg, S., Gerosa, G., 2018. Tropospheric ozone assessment report: Global ozone metrics for climate change, human health, and crop/ecosystem research. Elementa (Wash. D.C.) 6, 28. https://doi.org/10.1525/elementa.279.

Li, Y., Zeng, X., Liu, J., Liu, Y., Liu, S., Yin, P., Qi, J., Zhao, Z., Yu, S., Hu, Y., He, G., Lopez, A., Gao, G., Wang, L., Zhou, M., 2017. Can China achieve a one-third reduction in premature mortality from non-communicable diseases by 2030? BMC Med. 15 (1), 132. https://doi.org/10.1186/s12916-017-0894-5.

Li, J., Nagashima, T., Kong, L., Ge, B., Yamaji, K., Fu, J.S., Wang, X., Fan, Q., Itahashi, S., Lee, H.-J., Kim, C.-H., Lin, C.-Y., Zhang, M., Tao, Z., Kajino, M., Liao, H., Li, M., Woo, J.-H., Kurokawa, J., Wang, Z., Wu, Q., Akimoto, H., Carmichael, G.R., Wang, Z., 2019. Model evaluation and intercomparison of surface-level ozone and relevant species in East Asia in the context of MICS-Asia phase III – part 1: overview. Atmos. Chem. Phys. 19, 12993–13015. https://doi.org/10.5194/acp-19-12993-2019.

Liang, S., Li, X., Teng, Y., Fu, H., Chen, L., Mao, J., Zhang, H., Gao, S., Sun, Y., Ma, Z., Azzi, M., 2019. Estimation of health and economic benefits based on ozone exposure level with high spatial-temporal resolution by fusing satellite and station observations. Environ. Pollut. 255, 113267. https://doi.org/10.1016/j.envpol.2019.113267.

Lin, Y., Jiang, F., Zhao, J., Zhu, G., He, X., Ma, X., Li, S., Sabel, C.E., Wang, H., 2018. Impacts of O3 on premature mortality and crop yield loss across China. Atmos. Environ. 194, 41–47. https://doi.org/10.1016/j.atmosenv.2018.09.024.

Liu, Y., Wang, T., 2020. Worsening urban ozone pollution in China from 2013 to 2017 – part 1: the complex and varying roles of meteorology. Atmos. Chem. Phys. 20, 6305–6321. https://doi.org/10.5194/acp-20-6305-2020.

Liu, H., Liu, S., Xue, B., Lv, Z., Meng, Z., Yang, X., Xue, T., Yu, Q., He, K., 2018. Ground-level ozone pollution and its health impacts in China. Atmos. Environ. 173, 223–230. https://doi.org/10.1016/j.atmosenv.2017.11.014.

Lu, X., Hong, J., Zhang, L., Cooper, O.R., Schultz, M.G., Xu, X., Wang, T., Gao, M., Zhao, Y., Zhang, Y., 2018. Severe surface ozone pollution in China: a global perspective. Environ. Sci. Technol. Lett. 5 (8), 487–494. https://doi.org/10.1021/acs.estlett.8b00366.

Lu, X., Zhang, L., Wang, X., Gao, M., Li, K., Zhang, Y., Yue, X., Zhang, Y., 2020. Rapid increases in warm-season surface ozone and resulting health impact in China since 2013. Environ. Sci. Technol. Lett. 7 (4), 240–247. https://doi.org/10.1021/acs.estlett.0c00171.

Madaniyazi, L., Nagashima, T., Guo, Y., Pan, X., Tong, S., 2016. Projecting ozone-related mortality in East China. Environ. Int. 92–93, 165–172. https://doi.org/10.1016/j.envint.2016.03.040.

Maji, K.J., Namdeo, A., 2021. Continuous increases of surface ozone and associated premature mortality growth in China during 2015–2019. Environ. Pollut. 269, 116183. https://doi.org/10.1016/j.envpol.2020.116183.

Malashock, D.A., DeLang, M.N., Becker, J.S., Serre, M.L., West, J.J., Chang, K., Cooper, O.R., Anenberg, S.C., 2022. Estimates of Ozone Concentrations and Attributable Mortality in Urban, Peri-urban and Rural Areas Worldwide in 2019. 17, p. 054023. https://doi.org/10.1088/1748-9326/ac66f3.

Malley, C.S., Henze, D.K., Kuylenstierna, J.C.I., Vallack, H.W., Davila, Y., Anenberg, S.C., Turner, M.C., Ashmore, M.R., 2017. Updated global estimates of respiratory mortality in adults ≥ 30 years of age attributable to long-term ozone exposure. Environ. Health Perspect. 125, 087021. https://doi.org/10.1289/ehp1390.

Marco, A.D., Garcia-Gomez, H., Collalti, A., Khaniabadi, Y.O., Feng, Z., Proietti, C., Sicard, P., Vitale, M., Anav, A., Paoletti, E., 2022. Ozone modelling and mapping for risk assessment: an overview of different approaches for human and ecosystems health. Environ. Res. 211, 113048. https://doi.org/10.1016/j.envres.2022.113048.

Meehl, G.A., Tebaldi, C., Tilmes, S., Lamarque, J.F., Bates, S., Pendergrass, A., Lombardozzi, D., 2018. Future heat waves and surface ozone. Environ. Res. Lett. 13 (6), 064004. https://doi.org/10.1088/1748-9326/aabcdc.

REVIHAAP, 2013. Review of evidence on health aspects of air pollution – REVIHAAP Project technical report. Bonn, Germany: World Health Organization (WHO) Regional Office for Europe. http://www.euro.who.int/_data/assets/pdf_file/0004/193108/REVIHAAP-Final-technical-report-final-version.pdf.

Riahi, K., Van Vuuren, D.P., Kriegler, E., Edmonds, J., O'Neill, B.C., Fujimori, S., Bauer, N., Calvin, K., Dellink, R., Fricko, O., Lutz, W., Popp, A., Cuaresma, J.C., Kc, S., Leimbach, M., Jiang, L., Kram, T., Rao, S., Emmerling, J., Ebi, K., Hasegawa, T., Havlik, P., Humpenöder, F., Aleluia, L., Silva, D., Smith, S., Stehfest, E., Bosetti, V., Eom, J., Gernaat, D., Masui, T., Rogelj, J., Strefler, J., Drouet, L., Krey, V., Luderer, G., Harmsen, M., Takahashi, K., Baumstark, L., Doelman, J.C., Kainuma, M., Klimont, Z., Marangoni, G., Lotze-Campen, H., Obersteiner, M., Tabeau, A., Tavoni, M., 2017. The shared socioeconomic pathways and their energy, land use, and greenhouse gas emissions implications: an overview. Glob. Environ. Chang. 42, 153–168. https://doi.org/10.1016/j.gloenvcha.2016.05.009.

Shen, L., Jacob, D.J., Liu, X., Huang, G., Li, K., Liao, H., Wang, T., 2019. An evaluation of the ability of the ozone monitoring instrument (OMI) to observe boundary layer ozone pollution across China: application to 2005–2017 ozone trends. Atmos. Chem. Phys. 19, 6551–6560. https://doi.org/10.5194/acp-19-6551-2019.

Sicard, P., Agathokleous, E., Marco, A.D., Paoletti, E., Calatayud, V., 2021. Urban population exposure to air pollution in Europe over the last decades. Environ. Sci. Eur. 33, 28. https://doi.org/10.1186/s12302-020-00450-2.

Silva, R.A., West, J.J., Lamarque, J., Shindell, D.T., Collins, W.J., Dalsoren, S., Faluvegi, G., Folberth, G., Horowitz, L.W., Nagashima, T., Naik, V., Rumbold, S.T., Sudo, K., Takemura, T., Bergmann, D., Cameron-Smith, P., Cionni, I., Doherty, R.M., Eyring, V., Josse, B., MacKenzie, I.A., Plummer, D., Righi, M., Stevenson, D.S., Strode, S., Szopa, S., Zengast, G., 2016. The effect of future ambient air pollution on human premature mortality to 2100 using output from the ACCMIP model ensemble. Atmos. Chem. Phys. 16, 9847–9862. https://doi.org/10.5194/acp-16-9847-2016.

Travis, K.R., Jacob, D.J., Fisher, J.A., Kim, P.S., Marais, E.A., Zhu, L., Yu, K., Miller, C.C., Yantosca, R.M., Sulprizio, M.P., Thompson, A.M., Wennberg, P.O., Crounse, J.D., St. Clair, J.M., Cohen, R.C., Laughner, J.L., Dibb, J.E., Hall, S.R., Ullmann, K., Wolfe, G.M., Pollack, I.B., Peischl, J., Neuman, J.A., Zhou, X., 2016. Why do models overestimate surface ozone in the Southeast United States? Atmos. Chem. Phys. 16, 13561–13577. https://doi.org/10.5194/acp-16-13561-2016.

Turner, M.C., Jerrett, M., Pope, C.A., Krewski, D., Gapstur, S.M., Diver, W.R., Beckerman, B.S., Marshall, J.D., Su, J., Crouse, D.L., Burnett, R.T., 2016. Long-term ozone exposure and mortality in a large prospective study. Am. J. Respir. Crit. Care Med. 193, 1134–1142. https://doi.org/10.1164/rccm.201508-1633OC.

Turnock, S.T., Allen, R.J., Andrews, M., Bauer, S.E., Deushi, M., Emmons, L., Good, P., Horowitz, L., John, J.G., Michou, M., Nabat, P., Naik, V., Neubauer, D., O'Connor, F.M., Olivié, D., Oshima, N., Schulz, M., Sellar, A., Shim, S., Takemura, T., Tilmes, S., Tsigaridis, K., Wu, T., Zhang, J., 2020. Historical and future changes in air pollutants from CMIP6 models. Atmos. Chem. Phys. 20, 14547–14579. https://doi.org/10.5194/acp-20-14547-2020.

US Federal Register, 2015. National Ambient Air Quality Standards for Ozone, 40 CFR Part 50, 51, 52, 53, and 58, pp. 65292–65468.

van Vuuren, D.P., Kriegler, E., O'Neill, B.C., Ebi, K.L., Riahi, K., Carter, T.R., Edmonds, J., Hallegatte, S., Kram, T., Mathur, R., Winkler, H., 2014. A new scenario framework for climate change research: scenario matrix architecture. Clim. Chang. 122, 373–386. https://doi.org/10.1007/s10584-013-0906-1.

Wang, Y., Shen, L., Wu, S., Mickley, L., He, J., Hao, J., 2013. Sensitivity of surface ozone over China to 2000–2050 global changes of climate and emissions. Atmos. Environ. 75, 374–382. https://doi.org/10.1016/j.atmosenv.2013.04.045.

Wang, Y.L., Wild, O., Chen, X., Wu, Q., Gao, M., Chen, H., Qi, Y., Wang, Z., 2020. Health impacts of long-term ozone exposure in China over 2013–2017. Environ. Int. 144, 106030. https://doi.org/10.1016/j.envint.2020.106030.

Wang, F., Qiu, X., Cao, J., Peng, L., Zhang, N., Yan, Y., Li, R., 2021. Policy-driven changes in the health risk of PM2.5 and O3 exposure in China during 2013–2018. Sci. Total Environ. 757, 143775. https://doi.org/10.1016/j.scitotenv.2020.143775.

Wang, T., Xue, L., Feng, Z., Dai, J., Zhang, Y., Tan, Y., 2022. Ground-level ozone pollution in China: a synthesis of recent findings on influencing factors and impacts. Environ. Res. Lett. 17, 063003. https://doi.org/10.1088/1748-9326/ac69fe.

WHO, 2006. Air Quality Guidelines: Global Update 2005. Particulate matter, ozone, nitrogen dioxide and sulfur dioxide. World Health Organization Regional Office for Europe. http://www.euro.who.int/_data/assets/pdf_file/0005/78638/E90038.pdf?ua=1.

Xiao, Q., Geng, G., Xue, T., Liu, S., Cai, C., He, K., Zhang, Q., 2022. Tracking PM2.5 and O3 pollution and the related health burden in China 2013–2020. Environ. Sci. Technol. 56 (11), 6922–6932. https://doi.org/10.1021/acs.est.1c04548.

Xie, Y., Dai, H.C., Zhang, Y.X., Wu, Y.Z., Hanaoka, T., Masui, T., 2019. Comparison of health and economic impacts of PM2.5 and ozone pollution in China. Environ. Int. 130, 104881. https://doi.org/10.1016/j.envint.2019.05.075.

Xu, X.B., Lin, W.L., Xu, W.Y., Jin, J.L., Wang, Y., Zhang, G., Zhang, X.C., Ma, Z.Q., Dong, Y.Z., Ma, Q.L., Yu, D.J., Li, Z., Wang, D.D., Zhao, H.R., 2020. Long-term changes of regional ozone in China: implications for human health and ecosystem impacts. Elementa (Wash. D.C.) 8, 13. https://doi.org/10.1525/elementa.409.

Xue, T., Liu, J., Zhang, Q., Geng, G., Zheng, Y., Tong, D., Liu, Z., Guan, D., Bo, Y., Zhu, T., He, K., Hao, J., 2019. Rapid improvement of PM2.5 pollution and associated health benefits in China during 2013–2017. Sci. China Earth Sci. 62 (12), 1847–1856. https://doi.org/10.1007/s11430-018-9348-2.

Xue, T., Zheng, Y., Geng, G., Xiao, Q., Meng, X., Wang, M., Li, X., Wu, N., Zhang, Q., Zhu, T., 2020. Estimating spatiotemporal variation in ambient ozone exposure during 2013–2017 using a data-fusion model. Environ. Sci. Technol. 54, 14877–14888. https://doi.org/10.1021/acs.est.0c03098.

Yin, P., Brauer, M., Cohen, A.J., Wang, H., Li, J., Burnett, R.T., Stanaway, J.D., Causey, K., Larson, S., Godwin, W., Frostad, J., Marks, A., Wang, L., Zhou, M., Murray, C.J.L., 2020. The effect of air pollution on deaths, disease burden, and life expectancy across China and its provinces, 1990–2017: an analysis for the global burden of disease study 2017. Lancet Planet. Health 4, e386–e398. https://doi.org/10.1016/s2542-5196(20)30161-3.

Yin, H., Lu, X., Sun, Y., Li, K., Gao, M., Zheng, B., Liu, C., 2021. Unprecedented decline in summertime surface ozone over eastern China in 2020 comparably attributable to anthropogenic emission reductions and meteorology. Environ. Res. Lett. 16 (12), 124069. https://doi.org/10.1088/1748-9326/ac3e22.

Yue, H., He, C., Huang, Q., Yin, D., Bryan, B., 2020. A.: stronger policy required to substantially reduce deaths from PM2.5 pollution in China. Nat. Commun. 11 (1), 1462. https://doi.org/10.1038/s41467-020-15319-4.

Zhang, Q., Zheng, Y., Tong, D., Shao, M., Wang, S., Zhang, Y., Xu, X., Wang, J., He, H., Liu, W., Ding, Y., Lei, Y., Li, J., Wang, Z., Zhang, X., Wang, Y., Cheng, J., Liu, Y., Shi, Q., Yan, L., Geng, G., Hong, C., Li, M., Liu, F., Zheng, B., Cao, J., Ding, A., Gao, J., Fu, Q., Huo, J., Liu, B., Liu, Z., Yang, F., He, K., Hao, J., 2019. Drivers of improved PM2.5 air quality in China from 2013 to 2017. Proc. Natl. Acad. Sci. 116 (49), 24463–24469. https://doi.org/10.1073/pnas.1907956116.

Zhang, Z., Yao, M., Wu, W., Zhao, X., Zhang, J., 2021. Spatiotemporal assessment of health burden and economic losses attributable to short-term exposure to ground-level ozone during 2015–2018 in China. BMC Public Health 21, 1069. https://doi.org/10.1186/s12889-021-10751-7.

Zhang, X., Xu, W., Zhang, G., Lin, W., Zhao, H., Ren, S., Zhou, G., Chen, J., Xu, X., 2022. Discrepancies in ozone levels and temporal variations between urban and rural North China Plain: Possible implications for agricultural impact assessment across China. Elementa (Wash. D.C.) 10, 1. https://doi.org/10.1525/elementa.2022.00019.

Zheng, H., Zhao, B., Wang, S., Wang, T., Ding, D., Chang, X., Liu, K., Xing, J., Dong, Z., Aunan, K., Liu, T., Wu, X., Zhang, S., Wu, Y., 2019. Transition in source contributions of PM2.5

exposure and associated premature mortality in China during 2005–2015. Environ. Int. 132, 105111. https://doi.org/10.1016/j.envint.2019.105111.

Zhong, M., Chen, F.T., Saikawa, E., 2019. Sensitivity of projected PM2.5- and O3-related health impacts to model inputs: a case study in mainland China. Environ. Int. 123, 264–526. https://doi.org/10.1016/j.envint.2018.12.002.

Zhu, J., Liao, H., 2016. Future ozone air quality and radiative forcing over China owing to future changes in emissions under the representative concentration pathways (RCPs). J. Geophys. Res. Atmos. 121 (4), 1978–2001. https://doi.org/10.1002/2015JD023926.

Zhu, J., Liao, H., Mao, Y., Yang, Y., Jiang, H., 2017. Interannual variation, decadal trend, and future change in ozone outflow from East Asia. Atmos. Chem. Phys. 17, 3729–3747. https://doi.org/10.5194/acp-17-3729-2017.